



New Classes of Systematic Effects in Gas Spin Comagnetometers

D. Sheng,¹ A. Kabcenell,¹ and M. V. Romalis¹

Department of Physics, Princeton University, Princeton, New Jersey 08544, USA

(Received 15 July 2014; published 16 October 2014)

Atomic comagnetometers are widely used in precision measurements searching for spin interactions beyond the standard model. We describe a new ^3He - ^{129}Xe comagnetometer probed by Rb atoms and use it to identify two general classes of systematic effects in gas comagnetometers, one associated with diffusion in second-order magnetic-field gradients and another due to temperature gradients. We also develop and confirm experimentally a general and practical approach for calculating spin relaxation and frequency shifts due to arbitrary magnetic-field gradients.

DOI: 10.1103/PhysRevLett.113.163002

PACS numbers: 32.30.Dx, 06.30.Gv, 51.20.+d

Spin-dependent interactions are used by many low-energy experiments searching for new physics. Such experiments are often limited by noise and systematic effects associated with the magnetic field. To reduce these effects, a number of experiments rely on comagnetometers, first introduced in [1], that use two different spin species to measure magnetic fields in the same space and time. Examples of such experiments include searches for electric dipole moments of the neutron [2] and atoms [3,4], as well as searches for violation of local Lorentz invariance [5–7] and for new spin-dependent forces [8–11]. Comagnetometers also find practical applications in inertial rotation sensing [12,13].

Comagnetometers usually rely on fast atomic diffusion so that both spin species sample the same average magnetic field independent of its spatial profile. It is natural to consider effects that limit this property. Some such effects have been discussed in connection with neutron electric dipole moments experiments [14–16]; however, we are not aware of a general analysis in the gas-diffusion regime. Theoretical methods for the analysis of frequency shifts and spin relaxation due to magnetic-field gradients have recently attracted renewed interest for applications in precision measurements [17–23], expanding on earlier work [24,25]. Substantial research on similar problems in NMR is reviewed in [26].

In this Letter we use a ^3He - ^{129}Xe comagnetometer probed by Rb atoms to experimentally study the effects of magnetic-field gradients and temperature gradients. We find that second-order magnetic-field gradients cause shifts in the ratio of the ^3He and ^{129}Xe precession frequencies proportional to the third power of the gradient strength. We develop a new general approach for analysis of frequency shifts that does not rely on second-order perturbation theory and that can describe effects proportional to higher powers of the gradient strength. We expand spin polarization in diffusion eigenmodes of the Torrey equation [27], calculate the coupling matrix between the eigenmodes, and find its eigenvalues after truncating high-order modes suppressed

by diffusion. This approach works for arbitrary relative size of diffusion, gradient dephasing, and Larmor precession time scales if the motion of atoms is in the diffusion regime. A method similar to our approach is discussed in [28] for calculating spin relaxation due to linear gradients.

We also describe the effect of thermal diffusion [29] on comagnetometers, which, to our knowledge, has not been considered before. It causes a gradient in the relative concentration of the two spin species in the presence of a temperature gradient and results in a linear sensitivity of the spin-precession frequency ratio to the first-order magnetic-field gradient in the direction of the temperature gradient.

Comagnetometers using ^3He and ^{129}Xe , first introduced in [30], are a natural choice for precision measurements because both species have nuclear spin $I = 1/2$ and long spin coherence times. Previous experiments used inductive pickup coils [3,5] or superconducting quantum interference devices [11] to detect the dipolar magnetic field created by polarized ^3He and ^{129}Xe atoms outside of the cell. We use Rb atoms in the same cell to detect nuclear spins through their Fermi-contact interactions, which enhances the dipolar magnetic field by a factor of 5.6 for ^3He [31] and of 490 for ^{129}Xe [32]. However, spin interactions also cause shifts of the nuclear spin-precession frequencies due to the Rb polarization [33]. Therefore, our measurement procedure is designed to suppress the polarization of Rb during the free-precession measurement interval for nuclear spin. During this interval we turn off the lasers interacting with Rb atoms and apply a strong oscillating magnetic field at the Rb Zeeman resonance frequency to suppress Rb polarization [34] generated by spin exchange with ^{129}Xe [35].

The measurements are performed in a spherical 1.88-cm internal diameter cell made from GE180 aluminosilicate glass with 3.2 atm ^3He , 2.9 torr ^{129}Xe , 70 torr N_2 , and a droplet of natural abundance Rb with a small admixture of K. The droplet is used to plug the cell stem at its opening to prevent gas diffusion into the stem and improve cell sphericity. The surface spin relaxation time is about

50 sec for ^{129}Xe and much longer for ^3He . The cell is placed in a five-layer μ -metal shield and is held by a G10 rod attached to a three-axis translation stage outside of the shield to control its position relative to the magnetic field and gradient coils mounted inside the shield. The gradient coils are calibrated by measuring the frequency of nuclear spin precession as a function of cell position. A uniform bias field of 2.4 mG generated by a stable current source is applied in the \hat{z} direction. The cell is heated in a boron nitride oven to about 125 °C by ac electric currents; a separate stem heater is used to control the stem temperature independently. We monitor the temperatures of the cell stem, the bottom of the cell body, and the oven body with T-type thermocouples. The experimental setup is shown in Fig. 1(a).

We start by pumping Rb atoms for 20 min with a circularly polarized beam tuned to the Rb D_1 transition to

build up ^3He and ^3Xe polarization by spin exchange with Rb [36]. Then the pump beam is blocked and a rf pulse is applied in \hat{y} direction to tip both ^3He and ^{129}Xe spins by $\pi/2$. The frequency of nuclear spin precession is determined from two measurement pulses separated by a time T (30–50 sec) on the order of Xe T_2 [37]. Each measurement pulse uses a pump beam along the \hat{x} direction, whose polarization is modulated between left and right circular [38] at 200 Hz with an electro-optic modulator, and a linearly polarized probe beam along the \hat{z} direction. We measure the paramagnetic Faraday rotation of the probe beam [39] caused by Rb atoms that experience a tilt of the total magnetic-field direction due to the Fermi-contact interaction with transverse polarization of the nuclear spins. This measurement procedure minimizes Rb polarization along the bias field. The probe optical rotation signal is demodulated at 200 Hz by a lock-in amplifier before being recorded. In between the two measurement pulses all lasers are blocked, and we turn on a rf field along the \hat{x} direction with an amplitude of 4.8 mG and frequency of 1.5 kHz to depolarize Rb spins by saturating their Zeeman resonance. After the second measurement pulse, we recycle the ^3He polarization by applying a $\pi/2$ pulse with an appropriate phase to put ^3He spins back along the bias field. It is followed by a pulse of magnetic-field gradient to relax all transverse nuclear spin components and 1 min of optical pumping to build up the ^{129}Xe polarization before the next measurement cycle. Figure 1(b) shows the measurement sequence and an example of the signal recorded during the measurement pulse.

We fit the measured signals using the equation

$$\theta = A_{\text{Xe}} e^{-(t-t_m)/\tau_{\text{Xe}}} \sin[\omega_{\text{Xe}}(t - t_{0,\text{Xe}})] + b(t - t_m) + A_{\text{He}} e^{-(t-t_m)/\tau_{\text{He}}} \sin[\omega_{\text{He}}(t - t_{0,\text{He}})] + c, \quad (1)$$

where t_m is the center of the measurement pulse and $t_{0,\text{Xe}}$ ($t_{0,\text{He}}$) are the crossing-zero times of Xe (He). In each measurement pulse, lasting about 5 sec, there are several crossing-zero time points. We choose t_0 in the first pulse to be closest to the end of the pulse, and t_0 in the second pulse to be closest to the beginning of the pulse. The measurement pulses are also adjusted to turn them on and off close to the crossing-zero times for Xe. This minimizes the perturbation in the Larmor frequency for Xe, which is more sensitive to the presence of polarized Rb atoms. We find the Larmor frequency from $\omega = 2\pi N/\Delta t_0$, where Δt_0 is the difference of the t_0 for the two measurement pulses, and N is an integer number of precession periods in between. The transverse spin relaxation times τ_{Xe} and τ_{He} are determined from the ratio of the signal amplitudes in the two pulses. The ratio between ^3He and ^{129}Xe Larmor frequencies is

$$g = \frac{\omega_{\text{He}}}{\omega_{\text{Xe}}} = \frac{\gamma_{\text{He}} B + \Omega_E}{\gamma_{\text{Xe}} B + \Omega_E}, \quad (2)$$

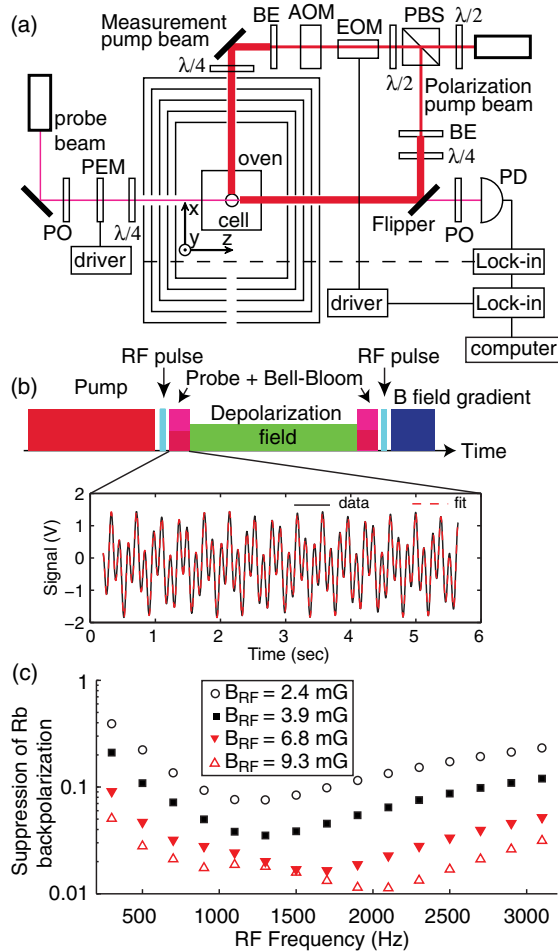


FIG. 1 (color online). (a) Top view of experimental setup. BE: beam expander, PBS: polarizing beam splitter, PO: polarizer, PD: photodiode, PEM: photoelastic modulator. (b) The sequence of the pulsed operation and an example of the signal recorded during the measurement pulse. (c) The fractional suppression of the Rb backpolarization generated by spin exchange with ^{129}Xe as a function of the amplitude and frequency of the depolarizing field.

where γ is the nuclear gyromagnetic ratio and Ω_E is the projection of the Earth's rotation onto the bias magnetic-field direction in the lab frame.

In Fig. 1(c) we show the dependence of the fractional suppression of the Rb backpolarization by ^{129}Xe on the frequency and amplitude of the depolarizing Zeeman rf field. The presence of this field slightly changes the gyromagnetic ratios, $\gamma' = \gamma_0 J_0(\gamma_0 B_d / \omega_d)$ [40], where J_0 is the zero-order Bessel function, γ_0 is the unperturbed gyromagnetic ratio, and B_d and ω_d are the magnetic-field amplitude and frequency of the depolarization field. This modification is different for ^3He and ^{129}Xe , and introduces a constant change in the frequency ratio, $g' = g - 6.3 \times 10^{-5}$. It is important that the depolarizing field does not have a rotating component, which would introduce a larger frequency shift. In a separate experiment we investigated the use of a depolarization field at the hyperfine resonance frequency of isotopically enriched ^{39}K atoms. This produces a similar suppression of electron polarization without a significant effect on nuclear spin-precession frequencies.

Frequency shifts due to linear magnetic-field gradients were first considered in [24] using second-order perturbation theory. Their analysis shows that the frequency ratio g does not change up to the second order in the gradient strength if the Larmor frequency is much faster than the diffusion time across the cell, $\omega \gg D/R^2$, where D is the diffusion constant and R is the cell radius. This condition is well satisfied in our experiment. However, in practical experiments, the field gradients are usually dominated by higher-order terms, either due to field coils or local magnetic impurities. To analyze higher-order gradients and higher powers of gradient strengths we developed a new method for calculating frequency shifts and relaxation rates in the gas-diffusion regime. We start with the Torrey equation [27] for the magnetization vector \mathbf{M} ,

$$\partial \mathbf{M} / \partial t = \gamma \mathbf{M} \times \mathbf{B} + D \nabla^2 \mathbf{M}. \quad (3)$$

In a spherical cell the magnetization is expanded in vector spherical harmonics and spherical Bessel functions, while the magnetic field is expanded in vector spherical harmonics, assuming no magnetic field sources inside the cell,

$$\mathbf{M}(\mathbf{r}, t) = \sum_{nljm} M_{nljm}(t) \mathbf{Y}_{jm}^l(\theta, \phi) j_l(k_{lm} r / R), \quad (4)$$

$$\mathbf{B}(\mathbf{r}) = \sum_{lm} B_{lm}(\sqrt{4\pi l / l!}) r^{l-1} \mathbf{Y}_{lm}^{l-1}(\theta, \phi). \quad (5)$$

Equation (3) is then converted to a system of linear differential equations for $M_{nljm}(t)$ using orthogonality and completeness of vector spherical harmonics and spherical Bessel functions. The equations are truncated at a maximum order in l and n because diffusion damps out higher-order terms. The eigenvalues of the resulting matrix

give the decay rates and frequencies of the normal diffusion modes. We evaluate the matrix symbolically as described in the Supplemental Material [41] and then find the eigenvalues numerically for a given diffusion constant and magnetic field specified by B_{lm} . We verified that this approach reproduces all results in [24]. It also remains valid when the rate of gradient dephasing is larger than the rate of diffusion across the cell, $\gamma \nabla B R > D/R^2$, where the perturbation theory in [24] breaks down. Spin relaxation on cell walls can be incorporated by modifying the boundary conditions used to determine the diffusion mode constants k_{lm} , as described in [41]. However, in a spherical cell the frequency ratio g is not affected by the surface relaxation if it is isotropic; this is because the average of the magnetic field over any spherical shell is equal to the field at the center of the shell [44]. To experimentally test our approach we measured the transverse spin relaxation rate due to first- and second-order gradients, $\delta B_z^{(1)} = G_1 z$ and $\delta B_z^{(2)} = G_2(z^2/2 - x^2/4 - y^2/4)$. In Fig. 2 we plot the difference between τ_{He}^{-1} (τ_{Xe}^{-1}) with and without the applied gradient. In our cell the diffusion constant for Xe is dominated by binary diffusion in He, while for He it is dominated by the self-diffusion constant; both are inversely proportional to the pressure of He. Using data from [45] we determine the ratio of the two diffusion constants $D_{^3\text{He}}/D_{\text{Xe}-^3\text{He}} = 3.38$ at 125 °C, after correcting for the isotopic mass difference between ^3He and ^4He . We checked the initial filling buffer-gas pressure in the cell by measuring the pressure broadening of the Rb D_1 line, which was recently calibrated in [46]. After correcting for the presence of N_2 , we find $D_{^3\text{He}} = 0.64 \text{ cm}^2/\text{sec}$ for our temperature and pressure based on data in [45]. There are no adjustable parameters in the comparison with the model in Fig. 2. To further verify our approach, we also extended the treatment in [24] to calculate the transverse relaxation due to a longitudinal gradient of order l , $\partial^l B_z / \partial z^l$, and find it agrees with our approach for high l [41]. For $l=2$ we find $1/T_2 = 11\gamma^2 R^6 (\partial^2 B_z / \partial z^2)^2 / 5880D$. Relaxation of spin-echo NMR signals due to quadratic gradients in one dimension was also experimentally studied in [47].

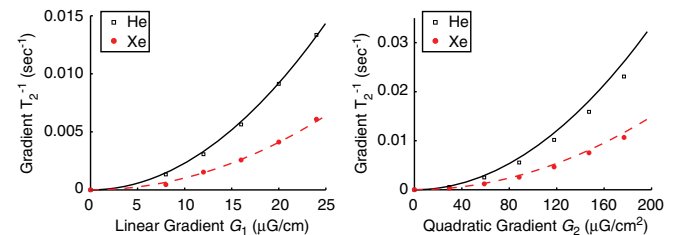


FIG. 2 (color online). Measurements of the transverse relaxation rate for ^3He and ^{129}Xe due to linear (left panel) and quadratic (right panel) magnetic-field gradients (points), together with results of the matrix analysis (lines) with no adjustable parameters.

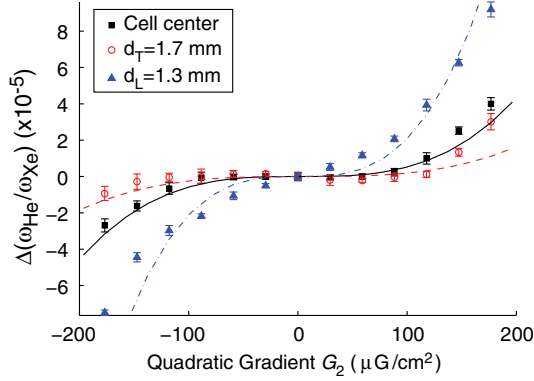


FIG. 3 (color online). Changes in the ratio of the spin-precession frequencies g due to the quadratic magnetic-field gradient $\delta B_z^{(2)}$. The three data presented are for the cell centered relative to the gradient coil (squares), displaced in the transverse direction by 1.7 mm (empty circles), and displaced along the \hat{z} direction by 1.3 mm (triangles). The lines are model predictions with no free parameters.

In Fig. 3 we show the shifts in the frequency ratio g due to the second-order gradient G_2 . We find that the second-order gradient causes a shift in g proportional to the third power of the gradient strength. This effect is due to nonuniform polarization of ^3He and ^{129}Xe spins caused by spatial variation in the gradient relaxation rate resulting in a shift of the “center of spin.” It cannot be described by second-order perturbation theory approaches, and it can cause systematic effects in precision measurements because it is odd in the gradient sign. It is also very sensitive to the position of the cell relative to the center of the gradient, as illustrated in Fig. 3. From our model and dimensional analysis we find that the fractional frequency shift $\delta\omega/\omega$ is proportional to $(\gamma/D)^2 G_2^3 R^{10}/B_0$, and that the effect on the frequency ratio g is suppressed in our case because the ratio of the diffusion constants is relatively close to $\gamma_{\text{He}}/\gamma_{\text{Xe}} = 2.75$.

When studying the response of the frequency ratio g to first-order gradients, we found that it is sensitive to the temperature gradients across the cell. This effect can be attributed to thermal diffusion—a gradient in the relative concentration of ^3He and ^{129}Xe spins due to a temperature gradient. The relative concentration gradient due to thermal diffusion is given by [29]

$$\frac{df_{\text{Xe}}}{dr} = -\alpha_T f_{\text{Xe}} f_{\text{He}} \frac{1}{T} \frac{dT}{dr}, \quad (6)$$

where the relative concentrations are $f_{\text{Xe}} = n_{\text{Xe}}/(n_{\text{He}} + n_{\text{Xe}})$, $f_{\text{He}} = n_{\text{He}}/(n_{\text{He}} + n_{\text{Xe}}) \approx 1$, and α_T is the thermal diffusion factor. A temperature gradient across the cell causes a nonuniform density of both helium and xenon to maintain a constant pressure, but for xenon the concentration is further increased in colder regions due to thermal

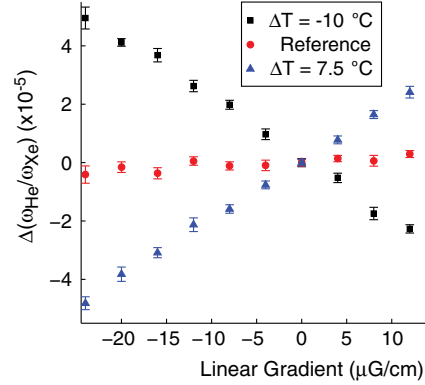


FIG. 4 (color online). Changes in the response of the frequency ratio g to a linear magnetic-field gradient $\partial B_z/\partial y$ in the presence of temperature gradient $\partial T/\partial y$ across the cell. ΔT denotes the temperature difference between the top and bottom of the cell.

diffusion. This causes a separation of the center of spin for the two species and a shift in the frequency ratio g for a linear field gradient parallel to the temperature gradient. In a spherical cell in a uniform temperature gradient the separation of the centers of spin is given by $d = \alpha_T R \Delta T / 10T$, where ΔT is the temperature difference across the cell. The thermal diffusion coefficient for small concentration of Xe in He is $\alpha_T = 1.06$ [45], and we calculate that for our conditions $d = 2.5 \times 10^{-4} \Delta T$ cm/K. Figure 4 shows the experimental measurements of the changes in g due to a vertical linear magnetic-field gradient $\partial B_z/\partial y$ for different vertical temperature gradients. We find that the sign of the shift changes with the sign of the temperature gradient and agrees with the sign of thermal diffusion. From the data we find $d = 2.0 \times 10^{-4} \Delta T$ cm/K, which is in good agreement with the calculation given the uncertainty in the temperature gradient of the gas in the cell.

In conclusion, we have described two new general classes of systematic effects that affect gas comagnetometers. One frequency shift is due to higher-order magnetic-field gradients, which have not been previously investigated, either experimentally or theoretically. We developed a high-order method to calculate the effects of field gradients, and we find that the frequency shift is proportional to the third power of the gradient strength. The second source of frequency shift is due to the thermal diffusion effect, which causes gradients in the relative concentration in the gases in the cell in the presence of a temperature gradient, resulting in sensitivity to first-order magnetic-field gradients. Identification of these systematic effects will be important for future precision measurements using comagnetometers, particularly for searches for spin-gravity coupling [48] and other interactions where signal reversal is difficult, as well as for their practical applications.

This work was supported by NSF and DARPA.

- [1] S. K. Lamoreaux, J. P. Jacobs, B. R. Heckel, F. J. Raab, and E. N. Fortson, *Phys. Rev. Lett.* **57**, 3125 (1986).
- [2] C. A. Baker *et al.*, *Phys. Rev. Lett.* **97**, 131801 (2006).
- [3] M. A. Rosenberry and T. E. Chupp, *Phys. Rev. Lett.* **86**, 22 (2001).
- [4] B. C. Regan, E. D. Commins, C. J. Schmidt, and D. DeMille, *Phys. Rev. Lett.* **88**, 071805 (2002).
- [5] D. Bear, R. E. Stoner, R. L. Walsworth, V. A. Kostelecký, and C. D. Lane, *Phys. Rev. Lett.* **85**, 5038 (2000).
- [6] J. M. Brown, S. J. Smullin, T. W. Kornack, and M. V. Romalis, *Phys. Rev. Lett.* **105**, 151604 (2010).
- [7] M. Smiciklas, J. M. Brown, L. W. Cheuk, S. J. Smullin, and M. V. Romalis, *Phys. Rev. Lett.* **107**, 171604 (2011).
- [8] B. J. Venema, P. K. Majumder, S. K. Lamoreaux, B. R. Heckel, and E. N. Fortson, *Phys. Rev. Lett.* **68**, 135 (1992).
- [9] G. Vasilakis, J. M. Brown, T. W. Kornack, and M. V. Romalis, *Phys. Rev. Lett.* **103**, 261801 (2009).
- [10] M. Bulatowicz, R. Griffith, M. Larsen, J. Mirjaniyan, C. B. Fu, E. Smith, W. M. Snow, H. Yan, and T. G. Walker, *Phys. Rev. Lett.* **111**, 102001 (2013).
- [11] K. Tullney *et al.*, *Phys. Rev. Lett.* **111**, 100801 (2013).
- [12] T. W. Kornack, R. K. Ghosh, and M. V. Romalis, *Phys. Rev. Lett.* **95**, 230801 (2005).
- [13] M. Larsen and M. Bulatowicz, *Proceedings of Frequency Control Symposium (FCS), 2012 IEEE International, Baltimore, MD, 2012* (2012).
- [14] P. G. Harris, J. M. Pendlebury, and N. E. Devenish, *Phys. Rev. D* **89**, 016011 (2014).
- [15] S. K. Lamoreaux *et al.*, *Europhys. Lett.* **58**, 718 (2002).
- [16] G. Baym, D. H. Beck, and C. J. Pethick, *Phys. Rev. B* **88**, 014512 (2013).
- [17] A. K. Petukhov, G. Pignol, D. Jullien, and K. H. Andersen, *Phys. Rev. Lett.* **105**, 170401 (2010).
- [18] R. Golub, R. M. Rohm, and C. M. Swank, *Phys. Rev. A* **83**, 023402 (2011).
- [19] W. Zheng, H. Gao, J.-G. Liu, Y. Zhang, Q. Ye, and C. Swank, *Phys. Rev. A* **84**, 053411 (2011).
- [20] S. M. Clayton, *J. Magn. Reson.* **211**, 89 (2011).
- [21] G. Pignol and S. Rocchia, *Phys. Rev. A* **85**, 042105 (2012).
- [22] M. Guigue, G. Pignol, R. Golub, and A. K. Petukhov, *Phys. Rev. A* **90**, 013407 (2014).
- [23] R. Golub and A. Steyerl, arXiv:1403.0871.
- [24] G. D. Cates, S. R. Schaefer, and W. Happer, *Phys. Rev. A* **37**, 2877 (1988).
- [25] D. D. McGregor, *Phys. Rev. A* **41**, 2631 (1990).
- [26] D. S. Grebenkov, *Rev. Mod. Phys.* **79**, 1077 (2007).
- [27] H. C. Torrey, *Phys. Rev.* **104**, 563 (1956).
- [28] A. V. Barzykin, *J. Magn. Reson.* **139**, 342 (1999).
- [29] K. E. Grew and T. L. Ibbs, *Thermal Diffusion in Gases* (Cambridge University Press, Cambridge, England, 1952).
- [30] T. E. Chupp, E. R. Oteiza, J. M. Richardson, and T. R. White, *Phys. Rev. A* **38**, 3998 (1988).
- [31] M. V. Romalis and G. D. Cates, *Phys. Rev. A* **58**, 3004 (1998).
- [32] Z. L. Ma, E. G. Sorte, and B. Saam, *Phys. Rev. Lett.* **106**, 193005 (2011).
- [33] S. R. Schaefer, G. D. Cates, T.-R. Chien, D. Gonatas, W. Happer, and T. G. Walker, *Phys. Rev. A* **39**, 5613 (1989).
- [34] F. Grossetête, *Compt. Rend.* **258**, 3668 (1964).
- [35] A. B. Baranga, S. Appelt, M. V. Romalis, C. J. Erickson, A. R. Young, G. D. Cates, and W. Happer, *Phys. Rev. Lett.* **80**, 2801 (1998).
- [36] T. G. Walker and W. Happer, *Rev. Mod. Phys.* **69**, 629 (1997).
- [37] D. Sheng, S. Li, N. Dural, and M. V. Romalis, *Phys. Rev. Lett.* **110**, 160802 (2013).
- [38] W. E. Bell and A. L. Bloom, *Phys. Rev. Lett.* **6**, 280 (1961).
- [39] W. Happer and B. S. Mathur, *Phys. Rev. Lett.* **18**, 577 (1967).
- [40] S. Haroche, C. Cohen-Tannoudji, C. Audoin, and J. P. Schermann, *Phys. Rev. Lett.* **24**, 861 (1970).
- [41] See Supplemental Material at <http://link.aps.org/supplemental/10.1103/PhysRevLett.113.163002> for calculation of the diffusion mode coupling matrix and relaxation rate due to high order gradients, which includes Refs. [42,43].
- [42] F. Masnou-Seeuws and M. A. Bouchiat, *J. Phys. (Paris)* **28**, 406 (1967).
- [43] D. A. Varshalovich, A. N. Moskalev, and V. K. Khersonskii, *Quantum Theory of Angular Momentum* (World Scientific, Singapore, 1988).
- [44] J. D. Jackson, *Classical Electrodynamics*, 2nd ed. (Wiley, New York, 1975), p. 184.
- [45] J. Kestin, K. Knierim, E. A. Mason, B. Najafi, S. T. Ro, and M. Waldman, *J. Phys. Chem. Ref. Data* **13**, 229 (1984).
- [46] K. A. Kluttz, T. D. Averett, and B. A. Wolin, *Phys. Rev. A* **87**, 032516 (2013).
- [47] P. Bendel, *J. Magn. Reson.* **86**, 509 (1990).
- [48] V. Flambaum, S. Lambert, and M. Pospelov, *Phys. Rev. D* **80**, 105021 (2009).